Deformed Penrose tilings

Philosophical Magazine,
Vol. 00, No. 00, DD Month 200x, 1–8

Deformed Penrose Tilings

T. R. WELBERRY*

Research School of Chemistry, Australian National University, Canberra, ACT 0200, Australia

B. SING

Fakultät für Mathematik, Universität Bielefeld, Universitätstrasse, 25, 33615 Bielefeld, Germany

(v3.1 released April 2006)

Monte Carlo (MC) simulation of a model quasicrystal (2D Penrose rhomb tiling) shows that the kinds of local distortions that result from *size-effect*-like relaxations are in fact very similar to mathematical constructions called *deformed model sets*. Of particular interest is the fact that these deformed model sets are pure *point-diffractive*, i.e. they give diffraction patterns that have sharp Bragg peaks and no diffuse scattering. Although the aforementioned MC simulations give diffraction patterns displaying some diffuse scattering, this can be attributed to the fact that the simulations include a certain amount of unavoidable randomness. Examples of simple *deformed model sets* have been constructed by simple prescription and hence contain no randomness. In this case the diffraction patterns show no diffuse scattering. It is demonstrated that simple deformed model sets can be constructed, based on the 2D Penrose rhomb tiling, by using deformations which are defined in terms of the local environment of each vertex. The resulting model sets are all topologically equivalent to the Penrose tiling (same connectedness), are perfectly quasicrystalline but show an enormous variation in the Bragg peak intensities. For the examples described, which are based on nearest-neighbour environments, 12 deformation parameters may be chosen independently. If more distant neighbours are taken into account further sets of parameters may be defined. One example of these simple deformed tilings, which shows great similarity to the *size-effect*-distorted tiling, is discussed in detail.

1 Introduction.

This study originated when the diffraction pattern of the decagonal quasicrystal, $Al_{71}Co_{13}Ni_{16}$, was published [1]. The zero-level section of this diffraction pattern is shown in Fig. 1a. Of particular interest is the very clearly delineated decagon feature indicated in the figure by the superimposed black line. The diffracted intensity (both diffuse scattering and Bragg peaks) on the outside (higher $\mathbf{Q}$) of this decagon is considerably higher than that on the inside. A second larger decagon (thin line) indicates a similar feature at higher Q, though here the intensity change is less pronounced. This feature is very reminiscent of features which occur in the diffraction patterns of disordered crystals, two examples of which are shown in Fig. 1b, and which are attributable to the atomic *size-effect* [2–5].

The atomic *size-effect* occurs in disordered crystals when a mixture of different atomic species, as for example in a disordered binary alloy, is allowed to relax locally. Neighbouring atoms tend to push apart if they are both larger than the average spacing or move closer together if they are smaller. Though it originates from near-neighbour interactions, the distortion spreads throughout the lattice and still has significant effects at quite large distances. The net result of the deviations from the perfectly periodic average lattice produces a series of sinusoidal modulations of the diffuse scattering. These have spacings of s, $2s$, $3s$ ...etc., where s is reciprocal to the real-space vector along which the interactions take place. The effect on the diffraction pattern is the characteristic abrupt change in intensity on going from one side of the Bragg position to the other, as shown schematically in Fig. 2. For a more detailed account of how these modulations arise from the basic diffraction equation see Welberry and Butler [6].

These effects in disordered crystals only affect the diffuse scattering intensites and the Bragg peaks are largely unaffected (the variations from the average lattice simply produce a modification of the Debye-Waller factor). In the quasicrystal pattern of Fig. 1 it is quite clear that both the diffuse scattering and the

*Corresponding author. Email: welberry@rsc.anu.edu.au

Philosophical Magazine
ISSN 1478-6435 print/ISSN 1478-6443 online
http://www.tandf.co.uk/journals
DOI: 10.1080/1478643YYxxxxxxxx

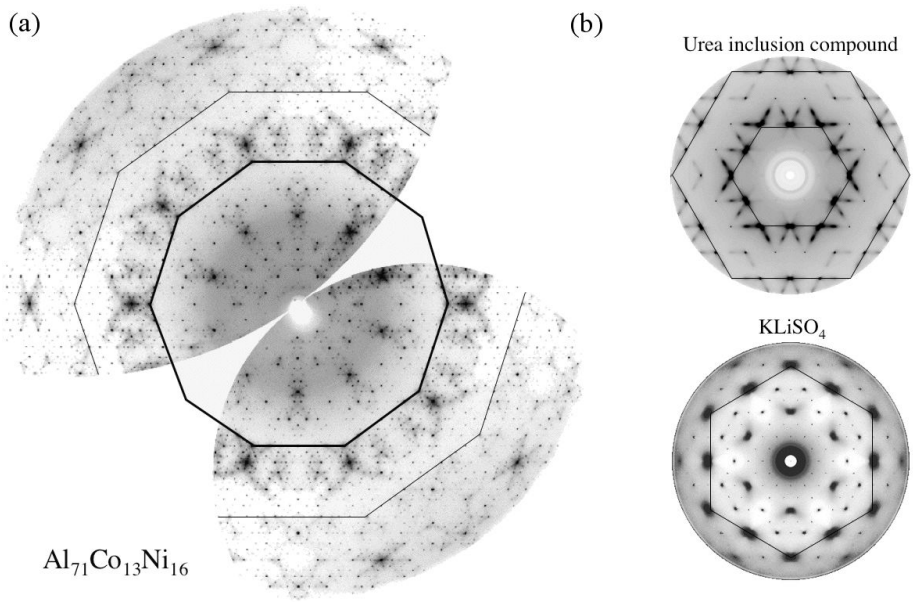

Figure 1. (a) The zero-level section of the decagonal quasicrystal $Al_{71}Co_{13}Ni_{16}$ [1]. Reproduced with kind permission of Prof. W. Steurer. (b) Two examples of real crystals showing similar asymmetry in the distribution of intensity that is caused by the atomic *size-effect* – a urea inclusion compound [4] and the tridymite analogue $KLiSO_4$ [5].

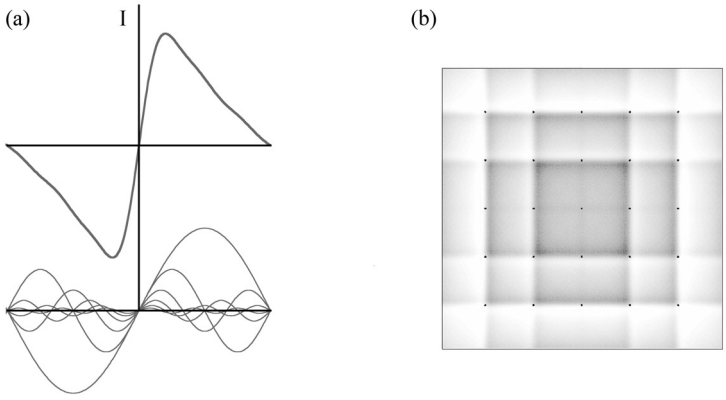

Figure 2. (a) Showing how the sum of sinusoidal modulations produces an asymmetric distribution of intensity across a Bragg peak position. (b) The intensity distribution calculated for a simple disordered alloy on a square lattice in which *size-effect* relaxation has been carried out. This example corresponds to the case where the larger atom has the larger scattering factor. If the larger atom has the smaller scattering factor the *size-effect* terms in the scattering equation change sign and the resulting pattern would have low intensity on the inside of the central square.

Bragg peaks show a similar type of asymmetry. Although many real quasicrystals contain some disorder and have diffraction patterns that contain diffuse scattering this is not a necessary requirement of a quasicrystal and an ideal quasicrystal will have Bragg peaks and no diffuse scattering just as a perfect crystal will. However, whereas in a perfect crystal a given atom will have exactly the same local environment in all unit cells, for a perfect quasicrystal a given type of atom will have many different local environments. For this reason it seems reasonable to suppose that there may be local relaxation in a quasicrystal which will differ from point to point according to the particular surroundings of a given type of atom, and this may give rise to an effect similar to the *size-effect* in crystals.

2 Distorted Penrose tiling.

In order to test this possibility Welberry and Honal [7] carried out a simple study in which a 2D Penrose rhomb tiling was distorted using Monte Carlo (MC) simulation by applying an artificial *size-effect*-like relaxation. In this, all of the rhomb-edge vectors were subjected to a force that attempted to make them

either longer or shorter depending on the two types of vertex they linked. In the description of the Penrose tiling used, the vertices were of four different types – circle, square, triangle and star as defined, for example, by Yamamoto and Ishihara [8]. Example regions of tiling in which these different symbols appear may be seen later (in Fig. 7). The *size-effect* algorithm tried to increase the length of circle-square and triangle-star vectors by 15% while decreasing the length of square-triangle vectors by the same amount. The result of this simple distortion is shown in Fig. 3. Here it is quite striking that the diffraction pattern shows the same kind of strong asymmetry between the outside and inside of a decagon as in the X-ray pattern of the real decagonal quasicrystal of Fig. 1. The Bragg intensities have been affected enormously, but in addition some diffuse scattering has appeared. Subsequently much of this diffuse scattering has been shown to originate from the residual randomness inherent in the MC simulation process [14]; see later also.

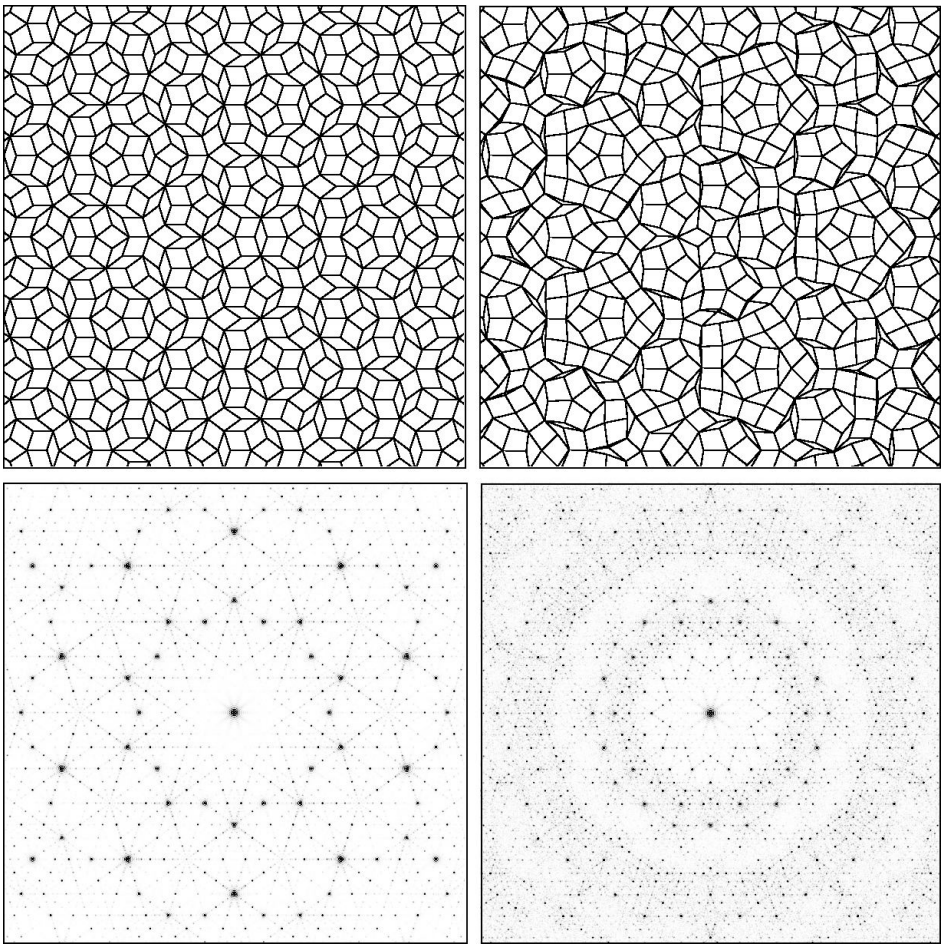

Figure 3. A small region of the 2D Penrose rhomb tiling together with its diffraction pattern both before and after *size-effect* relaxation. Note the diffraction pattern was obtained from a much larger region of the tiling than that shown, with a single atom placed at each vertex.

3 Deformed model sets.

The idea of deforming a tiling pattern is not new and was described relatively early in the development of quasicrystals (see for example p. 100 of the review of Janssen [9]). More recently Baake and co-workers have been involved in the development of mathematical models called *deformed model sets* [10–13] and this work has provided some rigorous proofs for such deformed tilings. In the present context a *model set* essentially means that it can be produced by the cut-and-project method from a higher-dimensional crystal. Model sets are pure point-diffractive; i.e. their diffraction patterns consist solely of Bragg peaks. The 2D Penrose rhomb tiling is an example of such a model set. Fig. 4 shows details of the cut-and-project

scheme for the Penrose rhomb tiling, when obtained by projection from the 5-dimensional hypercubic lattice. The projection window in the 3D internal space is the rhombic-icosahedron shown in Fig. 4a which in fact simply comprises the four pentagons A, B, C and D which contain all the points to be projected. Any point lying within one of the subregions of these pentagons shown in Fig. 4b results in a vertex of the rhomb tiling whose local environment is given by one of the configurations shown in Fig. 4c.

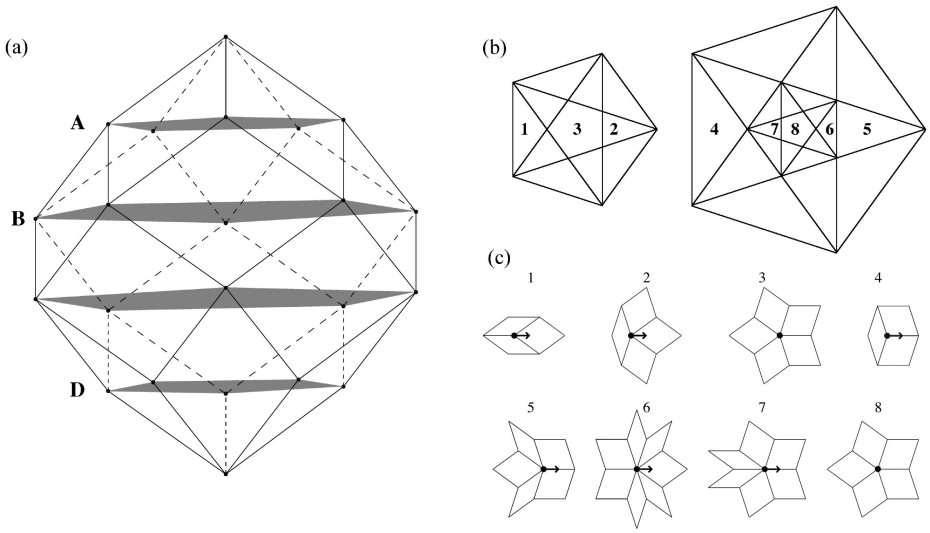

Figure 4. (a) The rhombic-icosahedron projection window of the 5-dimensional hypercubic lattice used to obtain the 2D Penrose rhomb tiling. Points lie only on the four pentagons labelled A, B, C, D. (b) The pentagons. A is related to D and B to C by inversion symmetry. The subregions of these pentagons labelled 1 to 8 give rise to the 8 different vertex configurations shown in (c).

A *deformed model set* is a model set in which each vertex in the tiling is displaced from its original (undeformed) position by an amount which is a continous function of the position in the window from which it has been projected. With the proviso of needing to be a continuous function the deformed model set will also be point-diffractive. It is therefore of interest to ask the question: is the distorted Penrose tiling that was produced by the *size-effect* relaxation, an example of a deformed model set? This question was addressed by Sing and Welberry [14] as described in the following section.

4 Size-effect distorted Penrose tiling as a deformed model set.

When a Penrose tiling is subject to the *size-effect* relaxation described above the end product is a set of cartesian coordinates for each of the vertices of the tiling. It is therefore a simple matter to compute the shift of each vertex, i, from the original perfect Penrose position to the new distorted position. We can thus assign both a magnitude, ν_i, and an orientation, ϕ_i, of this shift vector. If the distortion that has been induced by the *size-effect* algorithm is a continuous function in the internal space then the distorted tiling is in fact a deformed model set and will be point-diffractive. Fig. 5 shows a colour-coded (grey-scale) plot of ν_i for the large pentagon window. The figure on the left corresponds to coordinates from a single MC simulation. It is seen that for an appreciable proportion of the window the colour (grey-scale) is only slowly varying, while in other areas there is substantial and unpredictable noise. While the slowly varying areas seem to indicate that there is a lot of similarity to a deformed model set the noisy regions detract from this. The plot on the right of Fig. 5 was obtained from a set of vertex coordinates obtained by averaging over 500 different MC simulations (using different random number seeds). Now the variation of colour (grey-scale) is much smoother with considerably less of the unpredictable noise. Many smaller sub-regions of the pentagon are now clearly delineated. These sub-regions correspond to larger tile cluster configurations than the 8 basic configurations shown in Fig. 4c.

Similar plots to those shown in Fig. 5 were also obtained for vertices originating from the small pentagons of the projection window and also when the quantity being plotted was the shift vector orientation, ϕ_i. The conclusion from this work is that the tiling obtained from averaging the coordinates from 500 individual

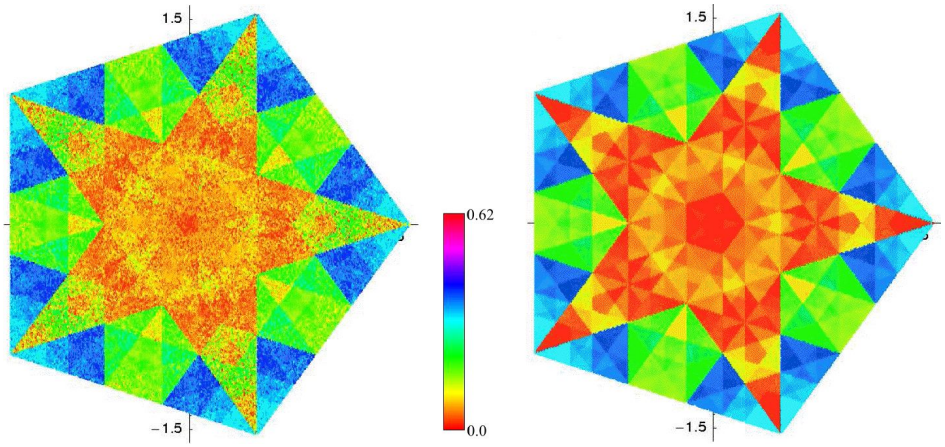

Figure 5. (a) Plot of the value of the displacement magnitude, ν_i, for points in the large pentagon of the projection window, for all vertices of a single MC simulation. (b) Corresponding plot for all vertices of a tiling obtained by averaging the coordinates from 500 MC simulations.

MC simulations is indeed very close to being a deformed model set. In any single MC run there is sufficient randomness remaining that the distribution cannot be considered to be a deformed model set. On close inspection this is seen to arise because of the particular way in which the *size-effect* distortion was achieved by applying forces along the rhomb-edges. For some particular local cluster configurations the result of such a relaxation is clearly defined, producing a local expansion or contraction of the structure as occurs in crystal lattices. However, for other configurations such as 1, 2, and 5 in Fig. 4c, the effect of trying to expand or contract rhomb-edges does not clearly define whether there will be a local expansion or contraction of the structure and the shift for such vertices is unpredictable and there is a large variation in different MC runs. When an average over many MC runs is carried out this greatly reduces the variation and results in the shifts for these vertices being more predictable. Nevertheless the tiling pattern for the averaged distorted Penrose tiling has a very similar appearance to that from a single MC run (see Fig. 6). The diffraction patterns too are very similar, although that from the averaged tiling has less diffuse scattering (see reference [14]).

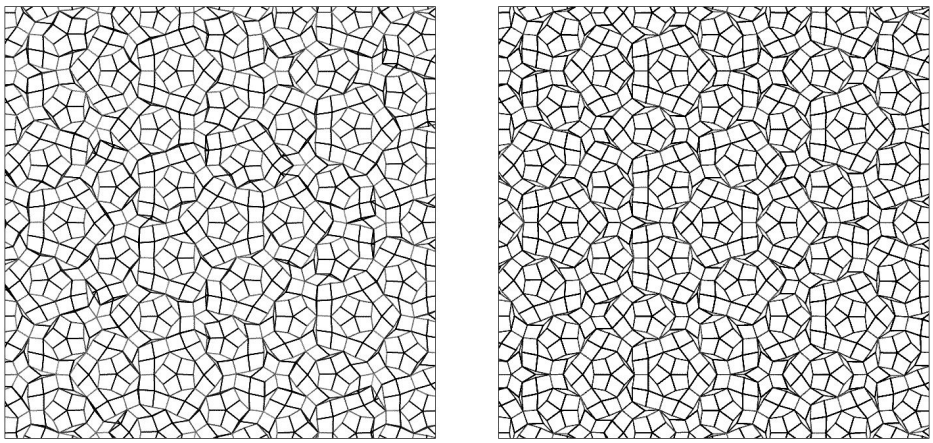

Figure 6. Comparison of the tiling patterns for a distorted Penrose tiling obtained from a single MC run (left) and the distorted tiling obtained from an average of 500 MC runs (right).

5 Simple deformed Penrose tilings.

The studies described above were directed towards trying to establish that the kind of distortion that is introduced into a quasicrystal by applying some kind of *size-effect* relaxation is in fact very similar to a deformed model set. In this section we perform the reverse operation by attempting to use deformed

model sets to generate directly quasicrystal realisations that approximate the example obtained by *size-effect* relaxation.

As a first approximation we take the 8 different types of subregion of the projection window pentagons shown in Fig. 4b and assume that the vertex displacements, ν_i, and their orientation, ϕ_i, originating from a given subregion are constant over the whole subregion. For each of the different types of vertex shown in Fig. 4c the $\phi_i = 0.0$ direction is defined as that given by the small arrows. In each case this direction has been chosen along a cluster symmetry direction. Cluster types 3 and 8 do not have an arrow since if either of these vertices were displaced the local symmetry would be broken. Nevertheless for the other six types of cluster it is possible to choose ν_i and ϕ_i quite independently. Fig. 7 shows the pattern of vertex displacements that originate from just one kind of pentagon subregion, namely subregion 4. The two parts of the figure show the pattern of vectors for a given choice of ν_4 but with two different values of ϕ_4, namely 0.0 deg and 22.5 deg.

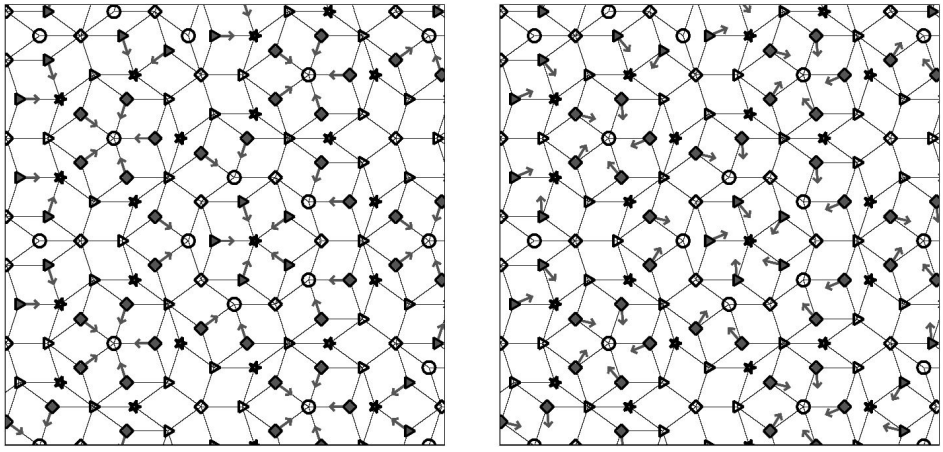

Figure 7. Showing the effect on the vertices of the displacement variable, ν_4, with two different values of the orientation, ϕ_4. Left $\phi_4 = 0.0$ deg. Right $\phi_4 = 22.5$ deg.

Fig. 7 shows just one example of the six possible displacement vectors, ν_i. The six ν_i together with their associated orientations, ϕ_i, make a total of 12 parameters that may be chosen completely independently. These provide a prescription for generating an enormous variety of different deformed tilings, all topologically equivalent to the Penrose pattern and all giving rise to pure point diffraction patterns. Three quite different examples are shown in Fig. 8. For each of these the orientation parameters ϕ_i were set to zero, hence they each preserve average mirror symmetry. For the example on the left, $\nu_1 = \nu_2 = \nu_4 = \nu_5 = \nu_6 = \nu_7 = -0.4$. The combined effect of these displacements has been to substantially enlarge what were originally the fat rhomb tiles (white) of the Penrose tiling and to close up what were originally thin rhombs (grey), giving a predominantly overall white appearance to the tiling. In contrast, for the middle example for which $\nu_1 = +0.8$; $\nu_2 = \nu_4 = +0.4$; $\nu_5 = \nu_6 = \nu_7 = 0.0$, the combined effect is to enlarge what were originally the thin rhombs (grey) and close-up what were originally fat rhombs (white), giving a predominantly overall grey appearance to the tiling. The third, rightmost example, for which $\nu_1 = 0.0$; $\nu_2 = +0.4$; $\nu_4 = -0.4$; $\nu_5 = \nu_6 = \nu_7 = 0.0$, was chosen as it gives a tiling pattern which is very similar to the tiling produced by the *size-effect* relaxation shown in Fig. 3.

Fig. 9 shows side-by-side the diffraction pattern of the third example from Fig. 8 and the pattern obtained earlier from the *size-effect* distorted tiling (Fig. 3). There is a lot of similarity of the two patterns in terms of the distribution of Bragg peak intensities, showing that the structures are similar. However, the decagonal feature, like that observed in the $Al_{71}Co_{13}Ni_{16}$ quasicrystal (Fig. 1) and which was the original motivation for this work, is clearly not well defined in the diffraction pattern of the deformed tiling though it is clearly present for the *size-effect* distorted pattern. Why should this be and what is the essential difference between the two structures?

In order to answer this question it should be borne in mind that the deformations used to produce the tilings of Fig. 8 were defined solely in terms of the near-neighbour tile configurations shown in Fig. 4c. There is no influence on the position of a given vertex from any more distant point. By contrast the distortion

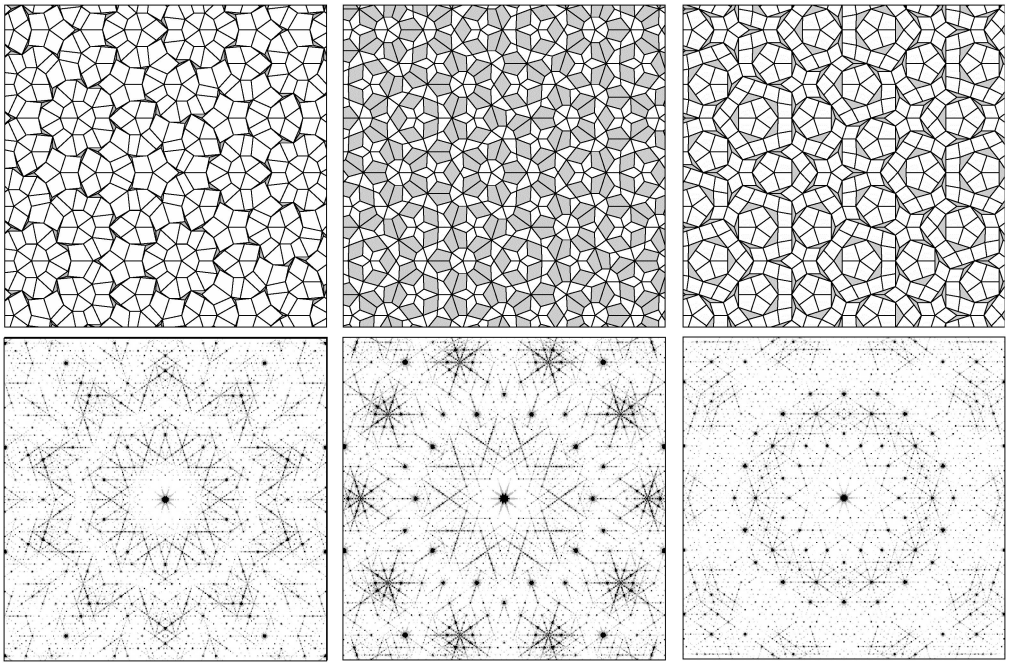

Figure 8. Three contrasting examples of *deformed* Penrose tilings and their diffraction patterns.

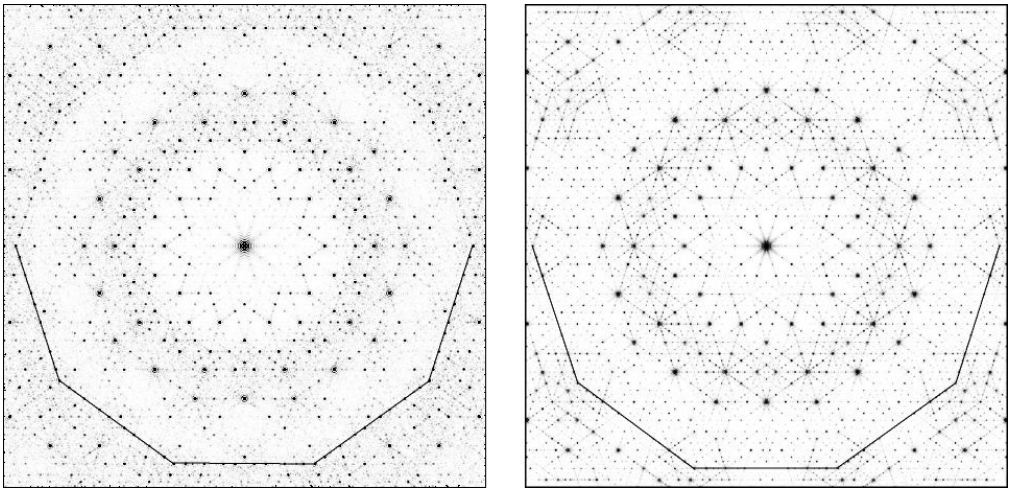

Figure 9. Comparison of the diffraction patterns of a size-effect distorted Penrose tiling (cf. Fig. 3) and a deformed Penrose tiling (cf. Fig. 8). Part of a decagon is superimposed on the lower half of the pattern to emphasise the decagonal feature referred to in the text.

produced by applying a *size-effect* algorithm, although having its origin in near-neighbour interactions, is propagated through the whole structure by successively more distant neighbours transmitting any displacement to which they themselves are subject. As was shown in Fig. 2 to get the characteristic abrupt change in intensity, between the inside and outside of the decagon, requires the sum of many sinusoidal terms which come from more and more distant neighbours and in the case of the *size-effect* distortion these are produced automatically. While the left pattern in Fig. 9 does appear to have been affected by many orders of sinusoidal terms, producing the abrupt and clearly delineated change of intensity, that on the right may be considered to have been modulated by only a single such term.

The simple deformations, which were defined by considering the 8 types of near-neighbour clusters shown in Fig. 4c, may thus be considered to be just the first-order term of a whole series of such deformations that may be defined by considering successively larger clusters. In the projection window this corresponds to dividing the 8 different subregions of the pentagons shown in Fig. 4b into smaller subregions. For each of these it is possible to define further parameters, ν_j and ϕ_j, say. These may be chosen quite independently of the first-order terms, ν_i and ϕ_i, and still produce point-diffraction patterns but in practice it might

be expected that they would be relatively minor perturbations to be applied to the first-order terms. That such smaller subregions are important in the *size-effect* example is shown by the clearly discernable subregions visible in Fig. 5. One consequence of considering larger clusters is that the displacement of vertices of types 3 and 8 will then not necessarily be zero.

6 Conclusion.

In this paper we have shown how application of a *size-effect* distortion to a simple model quasicrystal (Penrose tiling) can reproduce a distinctive diffraction feature similar to that observed in the decagonal quasicrystal, $Al_{71}Co_{13}Ni_{16}$. It has further been shown that the resulting distorted tiling closely resembles certain mathematical models called *deformed model sets* that have the property of being pure point-diffractive. Subsequent to this, some very simple deformed model sets have been investigated and the diversity of different deformed tilings and their diffraction patterns that may be obtained, even with such a simple prescription, has been illustrated. One such deformed tiling which has great similarity to the earlier *size-effect*-distorted tiling has been produced and arguments given that such a deformation represents a first-order term in a whole series of deformations that go to make up the *size-effect*-distorted tiling in which the effect of local strains extends throughout the structure.

7 Acknowledgement.

TRW would like to acknowledge the support of the Australian Research Council and the Australian Partnership for Advanced Computing. BS acknowledges financial support by the Cusanuswerk and the German Research Council, Collaborative Research Centre 701. BS thanks the Research School of Chemistry and the Cusanuswerk for financing a profitable stay and trip to Canberra. BS and TRW also thank Michael Baake for valuable discussions.

References

[1] M.A. Estermann, K. Lemster, T. Haibach, W. Steurer, Z. Kristallogr. **215** 584 (2000).
[2] B.E. Warren, B.L. Averbach, B.W. Roberts, J. Appl. Phys. **22** 1493 (1951).
[3] T.R. Welberry, J. Appl. Crystallogr. **19** 382 (1986).
[4] T.R. Welberry, S.C. Mayo, J. Appl. Crystallogr. **29** 353 (1996).
[5] T.R. Welberry, A.M. Glazer, J. Appl. Crystallogr. **27** 733 (1994).
[6] T.R. Welberry, B.D. Butler, J. Appl. Crystallogr. **27** 205 (1994).
[7] T.R. Welberry, M. Honal, Z. Kristallogr. **217** 422 (2002).
[8] A. Yamamoto and K.N. Ishihara, Acta Cryst. **A44** 707 (1988).
[9] T. Janssen, Physics Reports. **168** 55 (1988).
[10] A. Hof, in The Mathematics of Long-Range Aperiodic Order, edited by R. Moody (Kluwer, Dordrecht, 1997)., pp. 239–268.
[11] M. Baake and D. Lenz, J. Fourier Anal. Appl. **11** 125 (2005). http://arxiv.org/abs/math.MG/0404155
[12] M. Baake and B. Sing, Canad. Math. Bull. **47** 168 (2004). http://arxiv.org/abs/math.MG/0206098.
[13] G. Bernuau and M. Duneau, in Directions in Mathematical Quasicrystals, edited by M. Baake and R. Moody (AMS, Providence, RI., 2000)., pp. 43–60.
[14] B. Sing, T.R. Welberry, Z. Kristallogr. **221** 621 (2006).